INSTITUTE OF PHYSICS PUBLISHING PLASMA PHYSICS AND CONTROLLED FUSION

Plasma Phys. Control. Fusion **47** (2005) 635–643 doi:10.1088/0741-3335/47/4/004

Formation of convective cells during scrape-off layer biasing in the CASTOR tokamak

J Stockel[1], P Devynck[2], J Gunn[2], E Martines[3], G Bonhomme[4], I Voitsekhovitch[5], G Van Oost[6], M Hron[1], I Duran[1], P Stejskal[1], J Adamek[1], V Weinzettl[1] and F Zacek[1]

[1] Institute of Plasma Physics, Association Euratom/IPP.CR, AS CR, Prague, Czech Republic
[2] Association Euratom/CEA sur la fusion controlèe, Saint Paul Lez Durance, France
[3] Consorzio RFX, Associazione Euratom/ENEA sulla Fusione, Padova, Italy
[4] LPMI, UMR 7040 du CNRS, Université Henri Poincaré, Vandoeuvre-lès-Nancy, France
[5] Equipe Turbulence Plasma, LPIIM, Université de Provence, Marseille, France
[6] Department of Applied Physics, Gent University, Gent, Belgium

Received 14 July 2004, in final form 4 November 2004
Published 4 March 2005
Online at stacks.iop.org/PPCF/47/635

Abstract

We describe experiments with a biased electrode inserted into the scrape-off layer (SOL) of the CASTOR tokamak. The resulting radial and poloidal electric field and plasma density modification are measured by means of Langmuir probe arrays with high temporal and spatial resolutions. Poloidally and radially localized stationary structures of the electric field (convective cells) are identified and a related significant modification of the particle transport in the SOL is observed.

(Some figures in this article are in colour only in the electronic version)

1. Introduction

Understanding and controlling particle and heat transport at the tokamak edge is of primary importance in designing future large-scale experiments. However, requirements for the transport properties of the plasma inside and outside the last closed magnetic surface are contradictory. A low value of heat conductivity and consequent steep gradients of plasma pressure must be kept inside the last closed flux surface (LCFS) to achieve the best confinement. On the other hand, flat radial profiles (i.e. an amplified perpendicular transport) are required outside the LCFS (in the scrape-off layer (SOL)) to reduce the power density deposited to the first wall elements (limiters, divertor plates etc) thereby increasing their lifetime.

It is recognized that the edge transport inside the LCFS can be efficiently controlled by imposing electric fields, as reviewed for tokamaks [1, 2] and for stellarators [3]. In this case, an electrode is inserted inside the LCFS and biased with respect to the tokamak vessel. The magnetic surface associated with the electrode position is biased and a strongly sheared radial electric field $\boldsymbol{E}_r$ is formed between the electrode and the LCFS. Consequently, the plasma

slab between the electrode and LCFS is forced to rotate poloidally due to the $\boldsymbol{E}_\mathrm{r} \times \boldsymbol{B}_\mathrm{t}$ drift. When the rotation is sheared, the plasma turbulence, which is the dominant mechanism behind the anomalous transport in this region, is reduced. The edge transport barrier, characterized by a steep gradient of plasma density is formed in front of the LCFS.

Experiments involving the manipulation of fluctuations (and transport) inside the SOL are more scarce. A signature of broadening of the SOL profiles has been achieved by biasing a divertor plate in the JFT-2M tokamak [4]. Toroidally elongated structures of plasma potential have been formed in the SOL and the associated $\boldsymbol{E}_\perp \times \boldsymbol{B}_\mathrm{t}$ drift has been suggested as a mechanism of an enhanced transport [5]. Similar experiments were recently performed on the MAST spherical tokamak [6], where the divertor plates were biased as well. The formation of convective cells and a broadening of the power density profiles in the SOL were experimentally demonstrated [7].

An alternative approach has been successfully tested on the linear experiment Mirabelle [8], where a rotating pattern of ac voltage ($\sim$10 kHz) has been applied by means of a ring of electrodes surrounding the plasma column. A significant impact on drift wave turbulence was observed. This approach was adopted for toroidal geometry on CASTOR tokamak [9] and an increase of fluctuation levels was observed.

In this paper, we present results of experiments with biasing of an electrode immersed in the SOL of the CASTOR tokamak. The experimental set-up is described in section 2 in detail. Radial and poloidal distributions of plasma potential and the resulting modification of plasma density are shown in section 3. The results are summarized and future plans are outlined in section 4.

2. Arrangement of the experiment

2.1. Diagnostic tools

The experiments have been carried out on the CASTOR tokamak, which is a small-size torus with a major radius of 0.4 m and a minor radius of 0.1 m. The toroidal magnetic field is 1.3 T and the plasma current is varied between 5–10 kA. In the present experiment, the poloidal limiter with the radius $a = 58$ mm is equipped with 124 Langmuir probes, uniformly distributed around its circumference. This is apparent from the photo shown in figure 1. The individual tips are 2.5 mm long and spaced poloidally by $\sim$3 mm.

The rake probe, also seen in figure 1, is used to measure radial profiles of the edge plasma parameters in a single shot. The probe head is composed of 16 tips spaced radially by 2.5 mm and inserted into the edge plasma from the top of the torus, 180° toroidally away from the poloidal limiter. The signals are digitized with 1 MHz sampling rate and, 32 synchronized data acquisition channels are available.

The tips of both probe arrays can measure either the floating potential or the ion saturation current. The floating potential U_fl is related to the plasma potential φ by the formula $U_\mathrm{fl} = \varphi - \alpha T_\mathrm{e}$. Assuming a flat electron temperature profile, which is reasonable for the edge region of the CASTOR tokamak, gradients of floating potential can be considered as indicative of electric fields. Similarly, the ion saturation current gradient gives an estimate of the local plasma density gradient.

2.2. Asymmetry of the edge plasma

Simultaneous measurements with radial and poloidal probe arrays allow us to estimate asymmetries of the plasma column within the vacuum vessel of the CASTOR tokamak.

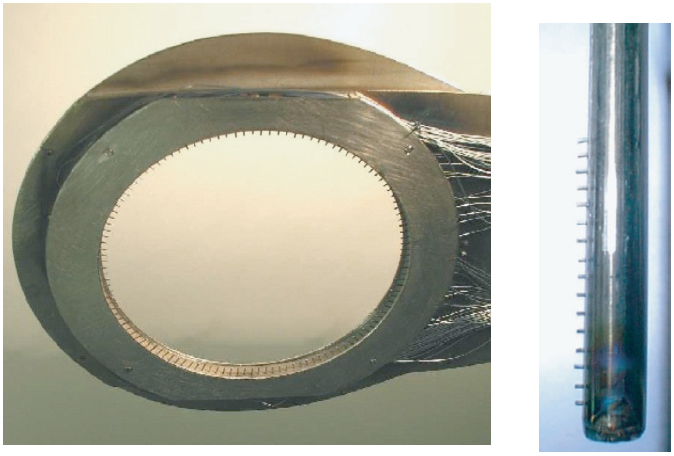

Figure 1. Probe arrays for spatially resolved measurements. Left picture—the poloidal limiter equipped with 124 Langmuir probes; right picture—the rake probe.

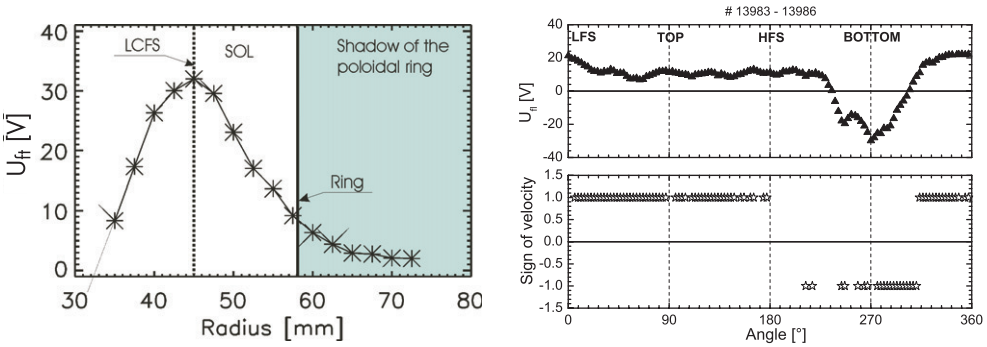

Figure 2. Typical distribution of the mean floating potential in ohmic discharge. Left—radial profile measured at the top of the torus by the rake probe. The radius of the poloidal limiter is marked. Right—poloidal distribution of floating potential and of the sign of the turbulence phase velocity as measured by the poloidal ring in four reproducible shots. The positive sign of the $\boldsymbol{E}_r \times B_t$ velocity corresponds to the poloidal propagation of turbulent structures in the region where $\boldsymbol{E}_r > 0$, i.e. inside the SOL.

First, let us discuss the distribution of the time-averaged floating potential U_{fl} in the radial direction that is measured by the rake probe during the ohmic phase of a discharge, which is shown in the left panel of figure 2.

As seen from the figure, the floating potential exhibits a maximum. The maximum floating potential marks the location where a $\boldsymbol{E} \times \boldsymbol{B}$ velocity shear is present. Therefore, it is assumed that such a maximum is located in the proximity of the LCFS [1]. The radial position of the LCFS at the top of the torus is at $r_s \sim 45$ mm in this particular case, which is noticeably deeper than the leading edge of the poloidal limiter $a = 58$ mm. Assuming a circular plasma cross section, the observed difference between the LCFS and limiter radius at the top of the torus is interpreted as a downward shift of the plasma column by ∼6–7 mm. It should be noted that previous measurements show that the floating potential decreases further and becomes negative at deeper insertions of the probe [1].

The right panel of figure 2 shows the distribution of the floating potential along the poloidal ring. As can be seen, the distribution at the top of the torus is relatively uniform, which means that the probes are located roughly on the same magnetic surface. On the other hand, the potential of the probes located at the bottom quarter of the poloidal circumference (in the range of poloidal angles 200–320°) is negative. The sign of the phase velocity of the turbulence computed from the cross-correlation of couples of probes adjacent to each other, also shown in figure 2, clearly shows that these latter probes are located on the opposite side of the velocity shear from the other ones. This suggests that they are effectively deeper than the LCFS.

These measurements are interpreted as follows. The SOL plasma is divided into two regions, regarding the parallel connection length L to a material surface, which is represented by the poloidal limiter:

- *Limiter shadow* is the region between the chamber wall and the leading edge of the poloidal limiter (58 mm $< r <$ 100 mm). The corresponding connection length is about one toroidal circumference, $L \sim 2\pi R$.
- *SOL* with a much longer connection length is formed at the upper part of the plasma column because of the vertical shift of the plasma. The connection length $L \sim q2\pi R$ is proportional to the local safety factor q (typically, $q = 6$–9 in CASTOR). The radial extent of the SOL is largest at the top of the torus and depends on the value of plasma displacement. This SOL is of similar magnetic configuration as that of a tokamak equipped with divertor or a toroidal limiter.

No magnetic measurements of the plasma position were available in this campaign.

3. Biasing of the SOL

The magnetic configuration described above is employed for the formation of stationary convective cells in the SOL of the CASTOR tokamak. The biasing electrode is immersed into the SOL from the top of the torus, 80° toroidally away from the limiter. The resulting positioning of the plasma column with respect to the poloidal limiter is schematically depicted in figure 3.

The graphite electrode has a mushroom-like shape. Its poloidal extent is 50 mm and the total collecting area ∼15 cm^2. The electrode is biased positively with respect to the tokamak vessel. The typical current to the electrode is in the range of 20–40 A at the biasing voltage $V_\mathrm{b} = 100$–200 V.

A rather complex picture is observed when the electrode is biased. This is apparent from figure 4, where the poloidal distribution of the mean floating potential in ohmic and biasing phases of a discharge is compared for $V_\mathrm{b} = 150$ V.

It is seen that the whole upper part of the torus is biased with respect to the ohmic level. Moreover, a strong poloidal modulation of the floating potential is observed in the range of poloidal angles $\theta = 0$–$200°$. The peaks are interpreted as a signature of a biased flux tube, which originates at the electrode and extends along the helical magnetic field line. The electrode current predominantly flows parallel to the magnetic field lines in the upstream and downstream direction and terminates on the electron and ion side of the bottom part of the poloidal limiter. It is interesting to note that the amplitude of the peaks strongly depends on the direction of the electrode current. The peaks corresponding to the downstream direction (located at $\theta_1 \sim 15°$ and $\theta_2 \sim 50°$) are significantly higher than those corresponding to the upstream direction ($\theta_{n\geqslant 3} > 90°$).

To check whether the biased flux tube really follows the local helicity of the magnetic field lines, a discharge with a plasma current ramp-down has been performed. The plasma

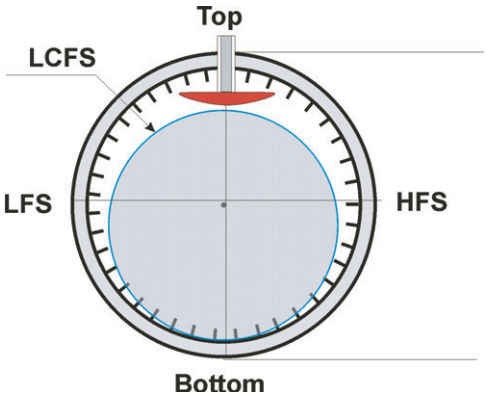

Figure 3. Schematic picture of the poloidal cross section of the CASTOR tokamak showing the respective position of the biasing electrode, plasma column and the poloidal limiter. The biasing electrode is located in the additional SOL.

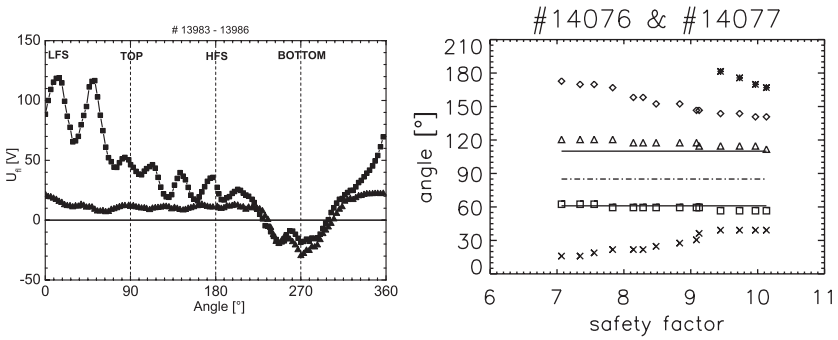

Figure 4. Left—poloidal distribution of the mean floating potential U_{fl} along the ring in ohmic (△) and biasing (□) phases, as measured in four reproducible discharges with a constant edge safety factor $q(a) \sim 8$. The poloidal position of the biasing electrode is marked by the bar. Right—poloidal position of five peaks (1–5) versus the edge safety factor, as measured during two reproducible shots with the current ramping down.

current decreases during the biasing period of the discharge, so that the local safety factor at the plasma edge increases from $q \sim 7$ to $q \sim 10$. The resulting angular position of five potential peaks (denoted by numbers 1–5) is shown in the right panel of figure 4. The angular difference between the peak positions decreases as expected. However, the angular positions of the peaks denoted as 2 and 3 are almost q-independent. These two peaks are the first projections (in the upstream and downstream direction) of the biasing electrode to the poloidal ring. Indeed, they cannot be found to be closer than the angular width of the biasing electrode, which is $\sim 50^{\circ}$. When the edge q-value would prescribe them to be closer, the smearing out due to the electrode itself will cause their apparent distance to be larger than or equal to 50° anyway. This can be better understood by looking at the projection of the biased tube on a poloidal plane, which is schematically depicted in figure 5.

The resulting perpendicular electric field is two-dimensional, having not only a radial, but also a poloidal component. The amplitude and even the sign of the poloidal electric field $\boldsymbol{E}_{\mathrm{pol}}$ changes with the poloidal angle. A possible consequence of this is the occurrence of a

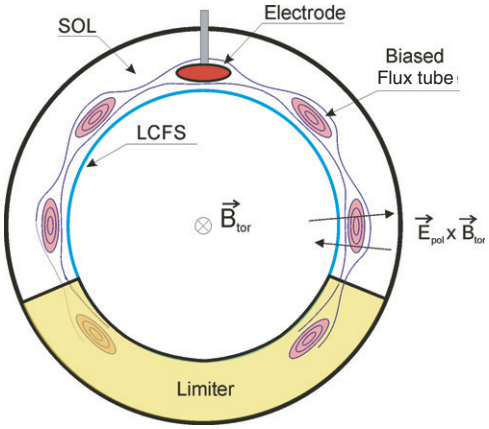

Figure 5. Projection of the biased flux tube originating at the electrode to a poloidal plane is shown schematically for $q_{edge} \sim 8$. Some equipotential surfaces are shown.

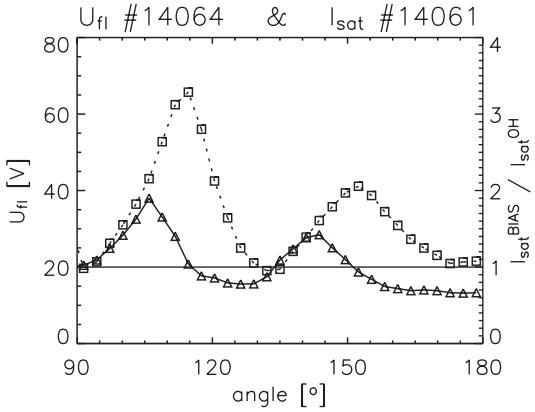

Figure 6. Poloidal distribution of the floating potential (□) and of the ion saturation current (△) along one quarter of the poloidal ring (high-field side—top). The ion saturation current is normalized to its ohmic value.

convective motion of the SOL plasma because of the $\boldsymbol{E}_{pol} \times \boldsymbol{B}_t$ drift directed either inward or outward according to the sign of $\boldsymbol{E}_{pol}$. In order to detect this effect, the tips of the poloidal ring have been used to measure either the floating potential or the ion saturation current in two subsequent reproducible discharges. A detailed distribution of these two quantities along one quarter of the poloidal ring, as allowed by the available data acquisition channels, is shown in figure 6. It is seen from the figure that the poloidal distribution of the ion saturation current (proportional to the plasma density) is modulated by the biasing with the same periodicity as the potential distribution, but is shifted poloidally. The ion saturation current (plasma density) increases at one side of the potential peaks, while it is reduced below the ohmic level on the other side. This suggests a variation of the edge density with the poloidal electric field. The poloidal electric field has been calculated as the difference of the floating potentials of adjacent tips divided by their distance and compared again with the poloidal distribution of the plasma density. The result is shown in figure 7.

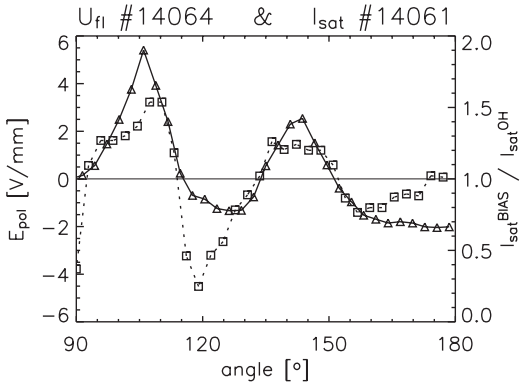

Figure 7. Distribution of the poloidal electric field (□) and the ion saturation current (△) along one quarter of the poloidal ring (high-field side—top). The ion saturation current is again normalized to its ohmic value.

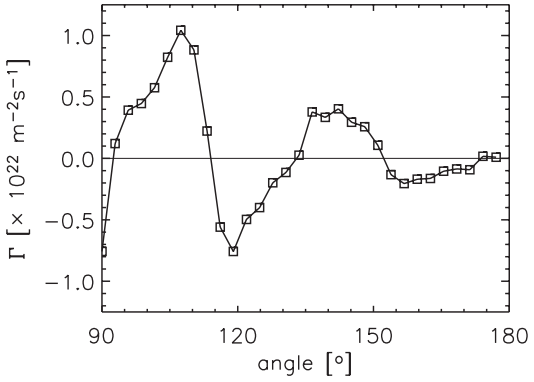

Figure 8. Distribution of the radial particle flux driven by the poloidal electric field along one quarter of the poloidal ring (high-field side—top).

It is evident that the relative change of the plasma density is practically proportional to the local value of the poloidal electric field. Some differences, which are observed in figure 7, can be attributed to an imperfect reproducibility of the analysed shots.

These measurements demonstrate a strong impact of the poloidal electric field on the particle transport in the plasma edge. Indeed, the radial particle flux driven by the poloidal electric field can be computed as

$$\Gamma \cong n v_{\boldsymbol{E}\times\boldsymbol{B}} = \frac{\boldsymbol{E}_{\mathrm{pol}} n}{B_{\mathrm{t}}}.$$

The result of such a calculation is shown in figure 8. A strong poloidal modulation of the particle flux is found. This is related to the oscillating behaviour found for the poloidal electric field. Furthermore, the effect is enhanced by the modulation of the density, which causes regions of denser plasma to move outward while regions of less dense plasma are pushed inwards.

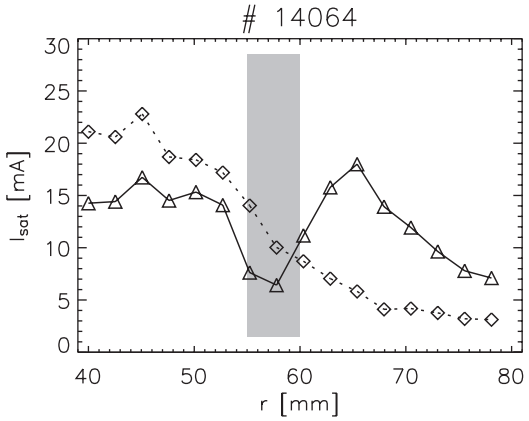

Figure 9. Comparison of the radial profile of the ion saturation current in the ohmic (- - - -) and in the SOL biasing (——) phases of the discharge. The grey bar marks the electrode position. The rake probe is located poloidally at $\theta \sim 90^{\circ}$, which corresponds to a region of positive electric field during the biasing phase.

The modulated radial particle flux can be compared with the average particle flux through the LCFS, denoted as Γ_g and estimated from the global particle balance from the following:

$$\Gamma_g \cong \frac{\bar{n}a}{2\tau},$$

where $\bar{n}$ is the volume average density, a is the radius of the LCFS and τ is the global particle confinement time. Using reasonable estimates of these quantities ($\bar{n} \approx 10^{19}\,\mathrm{m}^{-3}$, $a = 0.06\,\mathrm{m}$, $\tau \sim 10^{-3}\,\mathrm{s}$), we obtain $\Gamma_g \sim 3 \times 10^{20}\,\mathrm{m}^{-2}\,\mathrm{s}^{-1}$. The global particle confinement time has been evaluated by means of absolutely calibrated H_α-detectors. The computed average flux is considerably smaller than the peak values found in figure 8, implying that the biasing indeed has a very relevant effect on the overall particle balance of the SOL.

It is interesting to note that in some cases fluctuation driven fluxes measured by electrostatic probes in fusion devices appear to be too high to be consistent with the global particle balance [10, 11]. Large-scale convective cells naturally formed in the edge region may account for these apparent inconsistencies. Such cells are indeed predicted by fluid simulation including the effects of drifts [10] and have also been observed in the CCT tokamak [12].

The strong effect on the SOL equilibrium profile is further confirmed by measurements of the radial profile of the ion saturation current, obtained using the rake probe. Such measurements are shown in figure 9, both for the ohmic phase and during the SOL biasing. The density profile displays a strong depletion at the location of the electrode during the biasing phase. The density in front of this position is also reduced, whereas a density accumulation can be seen in the region between 60 and 70 mm, behind the electrode. This strong modification of the density profile is consistent with an increase of the particle flux at the radial location where the electrode is placed.

In fact, the density profile can be expected to be different at different poloidal locations, owing to the poloidal modulation of the particle flux. However, according to the tracing of the magnetic field lines the rake probe is located in a region of positive electric field, and therefore of positive particle flux, so that the effect observed on the density profile is indeed consistent with the local value of the particle flux.

4. Conclusions

With the help of a full poloidal ring of Langmuir probes, it has been possible to demonstrate the formation of stationary convective cells during SOL biasing in CASTOR. These are formed by the creation of a biased flux tube, which makes several toroidal turns in the SOL, according to the local safety factor value. As a consequence, not only the radial field, but also a rather strong poloidal electric field is formed at the magnetic surface associated with the biased electrode. This poloidal field changes its sign periodically along the poloidal circumference. Furthermore, the density is also poloidally modulated. The overall result is the creation of a pattern of particle flux with a strong modulation that makes it negative at some poloidal locations. This modulation can be seen as the formation of convective cells around the biased flux tube.

The results described in this paper are related to the SOL geometry of the CASTOR tokamak. In the present configuration, the downward shift of the plasma column allows flux tubes in the top part of the machine to describe several turns around the torus, which is an essential feature for the formation of the convective cells. Nevertheless, it is easy to envisage the application of the same technique to other geometries, including that of divertors.

It is important to emphasize that the technique described herein allows a strong increase of the transport in some regions of the SOL by the use of a single electrode with a limited extension in space. These results could have practical consequences for SOL engineering, and hence for exhaust in large-scale devices.

Acknowledgments

Authors are indebted to F Jiranek, V Havlik, K Rieger, M Satava and J Zelenka for the design, construction of diagnostics and technical assistance in the experiment. This work has been carried out with the support of the projects No 202/03/0786 (Grant Agency of the Czech republic) and No 2001-2056 (INTAS).

References

[1] Van Oost G, Stockel J, Hron M, Devynck P, Dyabilin K, Gunn J, Horacek J, Martines E and Tendler M 2001 *J. Fusion Phys. Res.* **4** 29
[2] Van Oost G *et al* 2003 *Plasma Phys. Control. Fusion* **45** 621
[3] Hidalgo C *et al* 2003 *Proc. 30th EPS Conf. on Controlled Fusion and Plasma Physics (St Petersburg, July 2003)* vol 27A (ECA) p 1.21
[4] Hara J *et al* 1997 *J. Nucl. Mater.* **241–243** 338
[5] Krlin L, Stockel J and Svoboda V 1999 *Plasma Phys. Control. Fusion* **41** 339
[6] Ryutov D D, Helander P and Cohen R H 2001 *Plasma Phys. Control. Fusion* **43** 1399
[7] Counsell G F, Cohen R H, Hellander P, Ryutov D D and the MAST team 2003 *Proc. 30th EPS Conf. on Controlled Fusion and Plasma Physics (St Petersburg, 2003)* vol 27A, p 3.202
[8] Schroeder C *et al* 2001 *Phys. Rev. Lett.* **86** 5711
[9] Stockel J *et al* 2002 *Proc. 19th Conf. on Fusion Energy (Lyon, France, 2002)* C&S PapersSeries 19/C, pp 1–11
[10] Garcia-Cortes I *et al* 2001 *J. Nucl. Mater.* **290–293** 604
[11] LaBombard B 2002 *Phys. Plasmas* **9** 1300
[12] Tynan G *et al* 1992 *Phys. Rev. Lett.* **68** 3032